UCLA
COMPUTATIONAL AND APPLIED MATHEMATICS

Regularization of Ill-Posed Problems Via the Level Set Approach

Eduard Harabetian
Stanley Osher

September 1995
(Revised December 1996)
CAM Report 95-41

Department of Mathematics
University of California, Los Angeles
Los Angeles, CA. 90024-1555

REGULARIZATION OF ILL-POSED PROBLEMS VIA THE LEVEL SET APPROACH

EDUARD HARABETIAN * AND STANLEY OSHER †

Abstract. We introduce a new formulation for the motion of curves in R^2, (easily extendable to the motion of surfaces in R^3), when the original motion generally corresponds to an ill-posed problem, such as the Cauchy-Riemann equations. This is, in part, a generalization of our earlier work in [6] where we applied similar ideas to compute flows with highly concentrated vorticity, such as vortex sheets or dipoles, for incompressible Euler equations. Our new formulation involves extending the level set method of [12] to problems in which the normal velocity is not intrinsic. We obtain a coupled system of two equations, one of which is a level surface equation. This yields a fixed grid, Eulerian method which regularizes the ill-posed problem in a topological fashion. We also present an analysis of curvature regularizations and some other theoretical justification. Finally, we present numerical results showing the stability properties of our approach and the novel nature of the regularization, including the development of bubbles for curves evolving under Cauchy-Riemann flow.

Key words.

AMS subject classifications.

1. Introduction. Our general problem is to move a curve $\Gamma_0 : (x_0(s), y_0(s))$ where s need not be arclength, through a system of partial differential equations

$$\begin{pmatrix} x_t \\ y_t \end{pmatrix} = \begin{pmatrix} v_1 \\ v_2 \end{pmatrix} = \vec{v}(t, x, y, x_s, y_s) \tag{1.1}$$

with periodic boundary conditions and initial conditions given by

$$\begin{pmatrix} x(s,0) \\ y(x,0) \end{pmatrix} = \begin{pmatrix} x_0(s) \\ y_0(s) \end{pmatrix}, \quad 0 \le s \le L \tag{1.2}$$

If the problem is Hadamard ill-posed, as for example in the initial value problem for the Cauchy-Riemann system:

$$\vec{v}(t, x, y, x_s, y_s) = \begin{pmatrix} -y_s \\ x_s \end{pmatrix} \tag{1.3}$$

one has to be content with computing the solution of a regularized problem.

In this work we consider the level set formulation of (1.1), i.e. the PDE associated with the function $\varphi(t, x, y)$, defined below, whose zero level set is the original curve (see [12]). If this PDE is approximated by a dissipative approximation, it provides a regularization which is closely related to the one obtained by adding a curvature term to the velocity of the original equation:

$$\begin{pmatrix} x_t \\ y_t \end{pmatrix} = \vec{v}(t, x, y, x_s, y_s) + \epsilon\kappa\vec{n} \tag{1.4}$$

where

$$\kappa = \frac{x_s y_{ss} - y_s x_{ss}}{(x_s^2 + y_s^2)^{3/2}}$$

is the curvature and

$$\vec{n} = \frac{1}{(x_s^2 + y_s^2)^{1/2}} \begin{pmatrix} -y_s \\ x_s \end{pmatrix}$$

is the normal.

In fact, away from singularities, (for example points where either $\nabla\varphi = 0$ or $\Gamma_s(t,s) = 0$, $\Gamma(s,t) = (x(t,s), y(t,s))$), the two regularizations are identical. This follows from the fact that in

* Department of Mathematics, University of Michigan, Ann Arbor, MI 48109. Research supported by NSF grant DMS-9204271 and AFOSR grant F49620-94-1-0215

† Department of Mathematics, University of California, Los Angeles, CA 90024. Research supported by NSF grant DMS–92-04942, ARO DAAH04-95-0155 and ARPA/ONR N00014-92-J-1890

the absence of singularities, if $\varphi(t,x,y)$ is the signed distance function to its zero level set, then $\Delta\varphi = -\kappa$.

We observe that the two regularizations are still identical at points where Γ is singular, such as the points where $\Gamma_s = 0$. For example, at such points, in the case of the Cauchy-Riemann equations (1.3), first there is a cusp, followed by the formation of a loop that changes the index in the curve. Consider the following exact solutions:

$$\begin{aligned} x(t,s) &= s + \beta\ sinh(\pi kt)cos(\pi ks) \\ y(t,s) &= t - \beta\ cosh(\pi kt)sin(\pi ks) \end{aligned} \tag{1.5}$$

with k a constant integer and β a real constant. At time $t = 0$ this is a smooth periodic curve of index 0. Singularities or kinks develop at the points where $cos(k\pi s) = 0$ at the critical time $t_{cr} = \frac{1}{\pi} sinh^{-1}(\frac{1}{\beta k\pi})$. These are the points where the curvature blows up. Past the critical time, the curve changes its index and loops develop. Both regularizations prevent these self-intersections (see Fig 2a).

There are topological reasons why this works. Consider the existence of smooth periodic solutions of the regularized Cauchy-Riemann equations in the polar variables θ, f,

$$\begin{aligned} \theta(s,t) &= arctan(\frac{y_s}{x_s}) \\ f(s,t) &= (x_s^2 + y_s^2)^{1/2} \end{aligned} \tag{1.6}$$

(see [12] for a discussion of this coordinate system for curves moving with curvature dependent velocity). The proof of existence with general smooth initial data, even for short time, is an open problem.

Assuming the existence result one can easily prove the topological regularization property and in particular that the winding number does not change. For instance, the winding number is given by the total change in θ along the curve (divided by 2π), and as long as θ remains smooth and periodic, that change remains 0.

Interestingly, the two regularizations differ however, at points where Γ is regular, but the level set function φ is singular, such as the points where different parts of the curve merge together without a change in index, forming a figure 8. In this case the solution $\Gamma(t,s)$, even with the curvature regularization, *does* allow the two parts of the curve to pass through each other, while φ prevents that from happening. This is consistent with the theory of Hamilton-Jacobi equations, in which multivalued solutions are replaced by single valued viscosity solutions. This is also illustrated in numerical results (see Fig. 3a-d).

Besides topological reasons, there are also analytical reasons why curvature regularizations work. Consider the example involving the regularized Cauchy-Riemann equations (which are nonlinear) and the behavior of small perturbations near the kinks. We show that the corresponding linearized problem is stable in the sense that no matter how small ϵ, *any* perturbation stays bounded as time increases. It is important to emphasize that the stability of the linear problem holds only when the linearization is done near kinks. Therefore, the above argument is formal, but serves to illustrate the particular nature of this regularization. In smooth regions without kinks, the curvature regularization is similar to other regularizations such as low-pass filters for which there is always a cut-off parameter depending on ϵ so that the Fourier modes below this cut-off in fact grow unboundedly in time. It is near kinks, or points of large curvature, that the regularization (1.4) is different, as we discussed above.

Curvature regularizations have been used before on other ill-posed problems such as denoising and deblurring in image processing applications [1, 14, 15]. The idea there is to process images by following the gradient flow for a particular functional. The Cauchy-Riemann equations (1.3), represent a gradient flow themselves, where the functional is the signed area enclosed by the curve:

$$A = \frac{1}{2}\int ydx - xdy$$

The gradient of A is interpreted in the following sense:

$$\lim_{\epsilon\to 0}\frac{d}{d\epsilon}A(\Gamma + \epsilon\tilde{\Gamma}) = \left(\nabla A(\Gamma), \tilde{\Gamma}\right) = \int \begin{pmatrix} -y_s \\ x_s \end{pmatrix} \cdot \begin{pmatrix} \tilde{x} \\ \tilde{y} \end{pmatrix} ds$$

Since curvature times the normal vector is the gradient of the length functional, the regularized Cauchy-Riemann equations represent the following gradient flow:

$$\begin{pmatrix} x_t \\ y_t \end{pmatrix} = \nabla(A - \epsilon L)$$

where L is the length of the curve:

$$L = \int (x_s^2 + y_s^2)^{1/2}$$

Geometrically, the Cauchy-Riemann system moves the curve in the direction of maximum increasing area while the curvature term compensates by making it move in the direction of maximum decreasing length.

There are numerical difficulties in solving (1.4) directly, caused by the stiffness of the curvature term, as has been observed by Sethian [16]. As regions of large curvature develop, discrete points on the curve converge, and any explicit time marching scheme will fail. It is then necessary to use complicated implicit schemes or regridding algorithms. One interesting and useful regridding scheme is due to Hou, Lowengrub and Shelley ([8]). We discuss its relevance and its relation to our approach in the next section. Their approach is successful in desingularizing a class of problems in which the curve develops a kink, but does not generally work for the strongly ill-posed problems discussed here.

A useful alternative is the level set method developed by Osher and Sethian in [12]. The original applications involved the motion of curves and surfaces whose speed depends on local curvature. Other applications and improvements continue to arise – see e.g. [1, 2, 4, 6, 9, 17, 18, 19]. Corresponding theoretical justification was given in [3, 5, 11] and elsewhere, and numerical schemes for the basic Hamilton-Jacobi equations were developed in [12, 13].

In the level set approach one embeds the curve $(x(s,t), y(s,t))$ in the level sets of a function $\varphi(t,x,y)$. One then determines the partial differential equation that φ must satisfy to be consistent with the motion of the curve. In the case in which the normal velocity is intrinsic (solely geometry or position based), this single equation which is of Hamilton-Jacobi type is sufficient to determine φ. For problems where the normal velocity is not intrinsic, such as the above Cauchy-Riemann equations, one equation is not sufficient.

In this work we first provide an extension to situations where the normal velocity need not be intrinsic and for which the problem written in Lagrangian (moving) coordinates is Hadamard ill-posed. The level set formulation leads to a coupled system of nonlinear equations which are solved on a fixed Eulerian grid by use of a standard dissipative scheme.

Our main observation is that this approach provides a regularization of the original problem which does not suffer from any stiffness side effects. As before, there are topological and analytical reasons for this regularization.

In addition, the linearized problem is *always* well-posed and quite simple in the direction of propagation normal to the level set, no matter what the equation (1.1) is. Overall, the problem may in general be ill-posed; however, there appears to be a tangential regularization through curvature as mentioned.

We have used as paradigms two ill-posed examples: the Cauchy-Riemann system, and in ([6]) the motion of a vortex sheet in two dimensional incompressible inviscid fluid flow. We shall also indicate how these methods can be applied to problems in three or higher dimensions.

The paper is organized as follows: in section 2 we introduce the level set formulation for an arbitrary moving front and determine when it is well-posed. We also analyze the stability of the regularized Cauchy-Riemann equations. In section 3 we show numerical results for the Cauchy-Riemann equations past the singularity time. The vortex sheet roll-up was computed in ([6]). Finally, we give the details of some of the more technical results in an Appendix.

2. The Level Set Method and Stability. In this section we introduce the level set formulation for an arbitrary moving front (1.1) (and its 3D analogue). We show that the system is always well-posed normal to the front, and verify it is well-posed overall if the original equations are well-posed. We then consider the curvature regularization and show that the regularized Cauchy-Riemann equations are linearly stable near kinks.

The level set method addresses the following problem. Given a region Ω (which might be multiply connected), we wish to move it normal to itself numerically, using a fixed (Eulerian) grid. The velocity is given by $\vec{v}$.

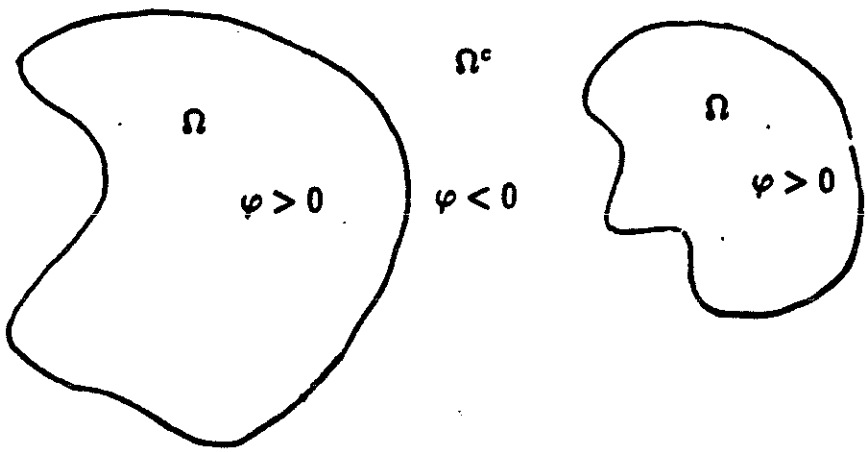

Figure 0

We construct an auxiliary function, $\varphi(x,t) > 0 \Leftrightarrow x \in \Omega$

$$\varphi(x,t) < 0 \Leftrightarrow x \in \Omega^c$$
$$\varphi(x,t) = 0 \Leftrightarrow x \in \partial\Omega$$
$$(all\ at\ time\ t)$$

Since $\varphi \equiv 0$ on $\partial\Omega$, we have

$$\varphi_t + \vec{v} \cdot \nabla\varphi = 0 \quad for \quad x \in \partial\Omega \tag{2.1}$$

and $\varphi \equiv 0$ characterizes $\partial\Omega$.

Generally, if $\vec{v} \cdot \vec{n}$ (for $\vec{n} = \frac{\nabla\varphi}{|\nabla\varphi|}|_{\varphi=0}$ the unit normal to $\partial\Omega$) is a function of the geometry, e.g. the curvature, the equation on $\partial\Omega$ becomes

$$\varphi_t + |\nabla\varphi| F(\kappa) = 0 \tag{2.2}$$

where

$$\kappa = -\nabla \cdot \left(\frac{\nabla\varphi}{|\nabla\varphi|} \right) \tag{2.3}$$

is the mean curvature of every level set of φ, particularly of $\partial\Omega$.

We extend (2.2) to be true throughout space and let the plotter find the resulting zero level set, which is $\partial\Omega$, at later times. Merging, pinching off, general topological changes and the development of singularities cause no difficulties here.

To see that singularities of $\partial\Omega$ do not affect the stiffness of (2.2) at least when F is linear in κ, note that

$$\kappa|\nabla\varphi| = -\vec{T} \cdot D^2(\varphi) \cdot \vec{T}$$

where

$$\vec{T} = \frac{1}{|\nabla\varphi|} \begin{pmatrix} \varphi_y \\ -\varphi_x \end{pmatrix} \tag{2.4}$$

and $D^2(\varphi)$ is the Hessian matrix of second derivatives of φ. Therefore, in analogy with the regular heat equation, the CFL condition for a time explicit marching scheme for (2.2) is of the form

$$const \frac{\Delta t}{\Delta x^2} \leq 1$$

where the constant does not dependent on how small $|\nabla\varphi|$ is. By contrast, in the Lagrangian framework where the variables are $x(s,t), y(s,t)$,

$$\kappa\vec{n} = \frac{1}{f^2}\vec{n} \cdot \begin{pmatrix} x_{ss} \\ y_{ss} \end{pmatrix} \vec{n}$$

where f is the arclength function given in (1.6) and $\vec{n}$ is the outward unit normal vector. The CFL condition for the corresponding problem is now

$$\frac{1}{f^2} \frac{\Delta t}{\Delta s^2} \leq 1$$

and problems arise near singularities, i.e. when f vanishes. Note that the two CFL expressions are "dimensionally" equivalent since

$$f^2 \Delta s^2 \approx dx^2 + dy^2$$

The stiffness is removed by approximating $dx^2 + dy^2$ on a fixed Eulerian grid.

We now turn to the general problem (1.1), where $\vec{v} \cdot \vec{n}$ may be parametrization dependent such as in the case of the Cauchy-Riemann system (1.3) where it is equal to f.

As usual, we defined $\varphi(t,x,y)$ so that

$$\begin{aligned} &\varphi(0,x,y) > 0 \ \ if \ (x,y) \ \varepsilon \ \Omega \\ &\varphi(0,x,y) < 0 \ \ if \ (x,y) \ \varepsilon \ \Omega^c \\ &\varphi(0,x_0(s),\ y_0(s)) \equiv 0 \end{aligned} \tag{2.5}$$

In addition, we now define the function $\psi(t,x,y)$ which evolves the parametrization of the curve in time. The function ψ is conjugate in the sense that the pair (φ,ψ) form an orthogonal coordinate system near the zero level set of φ. Initially

$$\psi(0,x(0,s),\ y(0,s)) \equiv s \tag{2.6}$$

and

$$\nabla\varphi \cdot (\nabla\psi)^* = \varphi_x\psi_y - \varphi_y\psi_x \neq 0 \tag{2.7}$$

at $t = 0$ on Γ_0.

We require, in addition to the usual criterion

$$\varphi(x(s,t),\ y(s,t),t) \equiv 0 \ \ for \ \ t > 0 \tag{2.8}$$

the additional criterion on the conjugate function

$$\psi(x(s,t),y(s,t),t) \equiv s \ \ for \ \ t > 0. \tag{2.9}$$

Differentiating both equations with respect to t leads us to two equations on $\Gamma(s,t)$

$$\varphi_t \ + \ \vec{v} \cdot \nabla\varphi \equiv 0 \tag{2.10}$$

$$\psi_t \ + \ \vec{v} \cdot \nabla\psi \equiv 0 \tag{2.11}$$

It remains to define x_s, y_s in terms of $\nabla\varphi$ and $\nabla\psi$ within the arguments of v in (2.10), (2.11). This is done on Γ by differentiating (2.8) and (2.9) with respect to s. We are led to

$$\varphi_x x_s + \varphi_y y_s = 0 \tag{2.12}$$

$$\psi_x x_s + \psi_y y_s = 1. \tag{2.13}$$

Solving this leads to

$$\begin{pmatrix} x_s \\ y_s \end{pmatrix} = [(\nabla\varphi) \cdot (\nabla\psi)^*]^{-1} \begin{pmatrix} -\varphi_y \\ \varphi_x \end{pmatrix} \tag{2.14}$$

on $\Gamma(s)$.

The quantity

$$(\nabla\varphi) \cdot (\nabla\psi)^* = \varphi_x\psi_y - \varphi_y\psi_x = -J$$

is the Jacobian of (φ,ψ) (the negative sign is there so that $J > 0$ in our applications). The variable J must not vanish in order for (2.14) to be well defined.

We replace (x_s, y_s) by this expression in the arguments of v in equation (2.10), (2.11), extend this to all space, and arrive at

$$\varphi_t \ + \ \vec{v}\left(x, y, \frac{\varphi_y}{J}, \frac{-\varphi_x}{J}\right) \cdot \nabla\varphi = 0 \tag{2.15}$$

$$\psi_t \ + \ \vec{v}\left(x, y, \frac{\varphi_y}{J}, \frac{-\varphi_x}{J}\right) \cdot \nabla\psi = 0 \tag{2.16}$$

This is our first level set formulation. It can be easily generalized to multidimensions, i.e. to the motion of an n dimensional surface in $n+1$ dimensions. In that situation, one has n conjugate functions $\psi_1, ..., \psi_n$, each satisfying an equation of the form (2.11). Equations such as (2.12),(2.13) can then be used to express the velocity in terms of gradients of φ, ψ_i.

We use this formulation in the Appendix to analyze the stability properties of the motion; however, its drawback is that the function ψ is not single valued on closed curves.

A more useful variable than ψ is J. To obtain the evolution equation for J, we let $\Phi(t,a) = (x,y)(t,a)$ be the trajectory of a point referenced by a under the flow, which implies

$$\begin{aligned} \varphi(t,\Phi(t,a)) &= \varphi(0,a) \\ \psi(t,\Phi(t,a)) &= \psi(0,a) \end{aligned}$$

i.e. φ and ψ are constant along flow trajectories. Differentiating with respect to a, and taking the determinant, we obtain

$$\left|\frac{\partial(\varphi,\psi)}{\partial(x,y)}\right| \left|\frac{\partial(x,y)}{\partial a}\right| = \left|\frac{\partial(\varphi_0,\psi_0)}{\partial a}\right|$$

Applying D_t (i.e. differentiating along the trajectory) to this equation, we obtain

$$D_t J \left|\frac{\partial(x,y)}{\partial a}\right| + J\, D_t \left|\frac{\partial(x,y)}{\partial a}\right| = 0$$

It is known [see [10], page 11] that

$$D_t \left|\frac{\partial(x,y)}{\partial a}\right| = (\nabla\cdot\vec{v}) \left|\frac{\partial(x,y)}{\partial a}\right|$$

Thus, we arrive at the following equation for J in Eulerian coordinates

$$J_t + \nabla\cdot(J\vec{v}) = 0 \tag{2.17}$$

This formula is also valid for the Jacobian of n functions in n space dimensions.

Let us remark at this point, that for divergence free flows (when $\nabla\cdot\vec{v}=0$), (2.17) implies that J is constant along particle trajectories. In particular, if J is a constant at time zero, it stays a constant for all time, and the equation (2.17) simply drops out. This fact was used in our work on vortex motion [6] to derive a simple algorithm for the evolution of a vortex sheet in an Eulerian framework.

We arrive therefore at the following system:

$$\varphi_t + \vec{v}\left(x,y,\frac{\varphi_y}{J},\frac{-\varphi_x}{J}\right)\cdot\nabla\varphi = 0 \tag{2.18}$$

$$J_t + \nabla\cdot\left(J\vec{v}\left(x,y,\frac{\varphi_y}{J},\frac{-\varphi_x}{J}\right)\right) = 0 \tag{2.19}$$

The distribution $\rho = J\delta(\varphi)$ represents the density near the level set and one easily verifies that ρ satisfies the same equation as J, i.e. it is conserved.

For the Cauchy-Riemann equations the system becomes

$$\varphi_t + \frac{|\nabla\varphi|^2}{J} = 0 \tag{2.20}$$

$$J_t + \Delta\varphi = 0 \tag{2.21}$$

The initial values corresponding to the example in (1.5) are

$$\begin{aligned} \varphi_0 &= y + \beta sin(\pi k x) \\ \psi_0 &= x \end{aligned}$$

Therefore $J_0(x,y) = 1$. We will discuss specific boundary conditions in the next section.

Another useful variable is

$$f = \frac{|\nabla\varphi|}{J} \tag{2.22}$$

Restricted to the curve Γ, f is the arclength variable $|\Gamma_s| = \sqrt{x_s^2 + y_s^2}$.

By substituting (2.22) into (2.17), we arrive at the following formulation involving the pair φ and f

$$\varphi_t + \vec{v}\left(x,y,f\frac{\varphi_y}{|\nabla\varphi|},f\frac{-\varphi_x}{|\nabla\varphi|}\right)\cdot\nabla\varphi = 0 \tag{2.23}$$

$$\left(\frac{|\nabla\varphi|}{f}\right)_t + \nabla\cdot\left(\frac{|\nabla\varphi|\vec{v}}{f}\right) = 0 \tag{2.24}$$

The equation (2.24) simplifies if the velocity is always normal to the curve, i.e.

$$\vec{v} = gf\vec{n} = gf\frac{\nabla\varphi}{|\nabla\varphi|}$$

for some function g. Substituting for $\vec{v}$ in (2.24), carrying out the differentiation, and using the equation for φ yields

$$-\frac{f_t}{f^2}|\nabla\varphi| - \frac{\nabla\varphi\cdot\nabla(gf)}{f} - \frac{g\nabla\varphi\cdot\nabla|\nabla\varphi|}{|\nabla\varphi|} + g\Delta\varphi + \nabla\varphi\cdot\nabla g = 0$$

or

$$\begin{aligned} f_t + \frac{fg\nabla\varphi\cdot\nabla f}{|\nabla\varphi|} &= gf^2\frac{\Delta\varphi|\nabla\varphi| - \nabla\varphi\cdot\nabla|\nabla\varphi|}{|\nabla\varphi|^2} \\ &= -gf^2\kappa(\varphi) \end{aligned}$$

where $\kappa(\varphi)$ is the curvature.

We therefore arrive at the following system in φ, f for the motion of a curve with purely normal velocity

$$\varphi_t + gf|\nabla\varphi| = 0 \tag{2.25}$$

$$f_t + fg\frac{\nabla\varphi\cdot\nabla f}{|\nabla\varphi|} = -gf^2\kappa(\varphi) \tag{2.26}$$

Equation (2.26) is more or less a Riccati equation for the "arclength" element f. Ill-posedness is reflected in the blow up ($f\to\infty$) or vanishing ($f\to 0$) of f, depending on the sign of κ, since f is non-negative.

In the special case of the Cauchy-Riemann equations, $g\equiv 1$.

As we mentioned before, extensions of this method applied to three equations in two space dimensions are (formally) very simple. For example, consider the motion of a surface $\vec{X}(t,u,v) = (x,y,z)(t,u,v)$, in which the velocity is purely normal, i.e.

$$\vec{X}_t = gf\vec{N}$$

Here f represents the area element, i.e.

$$f = |\vec{X}_u\times\vec{X}_v|$$

Using the same steps as above, it follows that the equations (2.25) and (2.26) represent a level set formulation for this motion, with κ the mean curvature of the surface. Details will be provided in future work.

In practice, the system (2.23)-(2.24) is approximated by a dissipative finite difference scheme such as the Lax-Friedrichs scheme. To be able to compute an ill-posed problem such as the Cauchy-Riemann system for large time, we explicitly add a curvature term. The curvature regularization (1.4) is implemented by modifying the equation for φ as follows:

$$\varphi_t + \left(\vec{v} + \epsilon\kappa(\varphi)\frac{\nabla\varphi}{|\nabla\varphi|}\right)\cdot\nabla\varphi = 0 \tag{2.27}$$

In practice, ϵ may be chosen to be proportional to the mesh size (see our numerical results in section 3).

The following results are obtained in the Appendix: The system (2.15)-(2.16) is always well-posed in the direction normal to the level curves φ = constant, in fact it is just linear advection with $\vec{v}$ "frozen", and it is well-posed if and only if the original system (1.1) is.

The level set formulation for the Cauchy-Riemann system (1.3) is an ill-posed system (see the Appendix), particularly in the direction tangent to the level curves. By adding a small curvature term to the motion, one obtains a tangential regularization near singularities. We wish to study the linearization of this system near a given solution.

We rewrite the Cauchy-Riemann equations in the variables $(\theta, \lambda = log(f))$ (see 1.6):

$$\theta_t = \lambda_s$$

$$\lambda_t = -\theta_s$$

We consider the following parabolic system:

$$\begin{aligned} \theta_t &= \lambda_s + \epsilon e^{-\lambda}(e^{-\lambda}\theta_s)_s \\ \lambda_t &= -\theta_s \end{aligned} \tag{2.28}$$

which is the curvature regularization.

For this analysis, we choose the particular solution

$$\begin{aligned} \theta_0 &= s \\ \lambda_0 &= -t \end{aligned} \tag{2.29}$$

The curvature $\kappa_0 = e^t$ is positive and becomes unbounded as t goes to infinity.

To study the behavior of nearby solutions we substitute:

$$\begin{pmatrix} \theta \\ \lambda \end{pmatrix} = \begin{pmatrix} \theta_0 \\ \lambda_0 \end{pmatrix} + \eta \begin{pmatrix} \theta_1 \\ \lambda_1 \end{pmatrix}$$

in (2.31) and collecting the $O(\eta)$ terms we obtain the linearized system:

$$\begin{pmatrix} \theta_1 \\ \lambda_1 \end{pmatrix}_t = \begin{pmatrix} 0 & 1-\alpha_\epsilon(t) \\ -1 & 0 \end{pmatrix} \begin{pmatrix} \theta_1 \\ \lambda_1 \end{pmatrix}_s + \alpha_\epsilon(t) \begin{pmatrix} \theta_1 \\ 0 \end{pmatrix}_{ss} \tag{2.30}$$

where

$$\alpha_\epsilon(t) = \epsilon \kappa_0 e^{-\lambda_0} = \epsilon e^{2t}$$

The main observation is that $\alpha_\epsilon > 1$ when $2t > log(1/\epsilon)$ and that the 2×2 matrix in (2.30) changes from a matrix with purely imaginary eigenvalues for $2t < log(1/\epsilon)$ to one with distinct real eigenvalues when $2t > log(1/\epsilon)$. This suggests the stability of the system (2.30) and the absence of any cutoff in frequencies. To obtain some estimates, it is enough to consider $t \geq t_0 > \frac{1}{2} log(1/\epsilon)$. Then, $\alpha_\epsilon - 1 > 0$ and we can symmetrize the system

$$\begin{pmatrix} \frac{\theta_1}{\alpha-1} \\ \lambda_1 \end{pmatrix}_t = \begin{pmatrix} 0 & -1 \\ -1 & 0 \end{pmatrix} \begin{pmatrix} \theta_1 \\ \lambda_1 \end{pmatrix}_s + \frac{\alpha}{\alpha-1} \begin{pmatrix} \theta_1 \\ 0 \end{pmatrix}_{ss} - \frac{\alpha_t}{(\alpha-1)^2} \begin{pmatrix} \theta_1 \\ 0 \end{pmatrix} \tag{2.31}$$

where we have omitted the ϵ subscript.

We proceed by multiplying (2.31) by

$$\begin{pmatrix} \frac{\theta_1}{\alpha-1} \\ \lambda_1 \end{pmatrix}$$

integrating in s and integrating by parts to obtain

$$\frac{1}{2} \frac{d}{dt} \int_{-\pi}^{\pi} \left[\left(\frac{\theta_1}{\alpha-1} \right)^2 + \lambda_1^2 \right] ds + \int_{-\pi}^{\pi} \frac{\alpha}{\alpha-1} (\theta_{1_s})^2 ds + \int_{-\pi}^{\pi} \frac{2\alpha}{(\alpha-1)^2} \theta_1^2 ds = 0$$

where we used $\alpha_t = 2\alpha$. Finally, integrating in time, from $t = t_0$ to $t = T$, and noting that $\alpha > 1$, we obtain

$$\begin{aligned} \int_{-\pi}^{\pi} \left[\left(\frac{\theta_1}{\alpha-1} \right)^2 + \lambda_1^2 \right] (T) ds &< M \\ \int_{t_0}^{T} \int_{-\pi}^{\pi} \frac{\alpha}{\alpha-1} (\theta_{1_s})^2 ds &< M \end{aligned}$$

where M is a constant dependent only on ϵ and the initial conditions, but independent of T. This gives a uniform bound in time for λ_1 and suggests a decay in θ_{1_s}.

We conclude this section with an observation which concerns an earlier case due to Osher and Sethian [12] of a simple problem which is (mildly) ill-posed in the Lagrangian framework but which becomes well-posed in the level set framework using the notion of viscosity solution.

We consider the simple problem of a front moving normal to itself with constant (say unit) velocity. This becomes (2.25) with $g = \frac{1}{f}$. The level set formulation decouples, and we get the Hamilton-Jacobi equation

$$\varphi_t + |\nabla \varphi| = 0 \tag{2.32}$$

whose viscosity solutions are the limits of positive curvature: for $\epsilon > 0$ small:

$$\varphi_t + |\nabla \varphi| = \epsilon |\nabla \varphi| \left(\nabla \cdot \frac{\nabla \varphi}{|\nabla \varphi|} \right). \tag{2.33}$$

The viscosity solution kills small scale oscillations, captures kinks, and the finite difference approximations used are not stiff [12].

To show the ill-posedness of the Lagrangian method we can use θ and f (see (1.6)) arriving at

$$f_t = \theta_s \tag{2.34}$$

$$\theta_t = 0. \tag{2.35}$$

This is a hyperbolic system with 0 as double eigenvalue – it has a Jordan block. The exact solution is

$$\theta \equiv \theta_0(s) \tag{2.36}$$

$$f \equiv f_0(s) + t\theta_0'(s). \tag{2.37}$$

This will cause f to turn negative if θ_0 is ever decreasing – particles intersect. It is also (mildly) classically ill-posed. The blow-up is linear in the Fourier frequency, rather than exponential.

Both methods are limits of positive curvature. The Lagrangian formulation is

$$\begin{aligned} x_t &= -\frac{y_s}{f}(1 - \epsilon\kappa) \\ y_t &= \frac{x_s}{f}(1 - \epsilon\kappa). \end{aligned} \tag{2.38}$$

This is a very stiff system, very difficult to compute with for ϵ small, [16] while (2.33) is robust and can be computed uniformly in ϵ. However, a new idea of Hou, Lowengrub and Shelley [8] can be used to remove the stiffness here. In this case, the idea amounts to adding tangential velocity to the original system, of the form

$$T = S - \theta$$

$S = 2\pi s/L(t)$ where s = arclength, and $L(t)$ = total length of the curve. The normal velocity is unchanged and the motion of the curve is unaffected as long as it stays smooth. The resulting motion is governed by

$$\begin{aligned} \theta_t - \frac{2\pi}{L(t)}(\theta - s)\theta_s &= 0 \\ L(t) &= L(0) + 2\pi t \end{aligned}$$

This equation predicts a shock in θ if the initial curve is nonconcave, which is correct. Also, adding ϵ curvature, for $\epsilon > 0$ to the motion, and letting $\epsilon \to 0$ can be shown to give the entropy condition satisfying the criterion for the jump in θ, [7].

The level set method for curvature dependent motion also yields a formulation involving θ and s, for s arc length.

We begin with the equation

$$\varphi_t = |\nabla\varphi| F\left(-\nabla \cdot \left(\frac{\nabla\varphi}{\nabla\psi}\right)\right), \quad F'(0) \leq 0,$$

and follow the motion of the zero level set of φ.

By rotating coordinates, if necessary, we can view this locally as a graph.

$$\varphi = y - \psi(x, t)$$

arriving at

$$\psi_t = -\sqrt{1 + \psi_x^2}\, F\left(\frac{\psi_{xx}}{(1 + \psi_x^2)^{3/2}}\right).$$

We also have

$$\theta = \tan^{-1}(\psi_x),$$

thus

$$\begin{aligned} \theta &= \frac{\psi_{xt}}{1 + \psi_x^2} = \frac{1}{1 + \psi_x^2}\frac{\partial}{\partial x}\left(-\sqrt{1 + \psi_x^2} F\left(\frac{\psi_{xx}}{(1 + \psi_x^2)^{3/2}}\right)\right) \\ &= \frac{-\psi_{xx}\psi_x}{(1 + \psi_x^2)^{3/2}} F\left(\frac{\psi_{xx}}{(1 + \psi_x^2)^{3/2}}\right) - \frac{1}{\sqrt{1 + \psi_x^2}}\frac{\partial}{\partial x} F\left(\frac{\psi_{xx}}{(1 + \psi_x^2)^{3/2}}\right) \end{aligned}$$

Thus we arrive at

$$\theta_t + (\tan\theta)\theta_s F(\theta_s) = -\frac{\partial}{\partial s}F(\theta_s).$$

This resembles the results obtained in [7], at least for $|\theta|$ bounded away from $\frac{\pi}{2}$ or for $|\theta_x|$ bounded i.e., (as long as the curve remains a graph).

The general procedure of regridding in [8] works only if the normal velocity of the curve is intrinsic - independent of the parametrization used. This rules out most of the ill-posed examples. However, the important case of vortex sheets for the incompressible Euler equations fits here, and was done in [7].

3. Numerical Results. In this section we present numerical results for the Cauchy-Riemann equations with different sets of initial data.

In the first set of experiments, we chose initial data corresponding to a sinusoidal curve plus noise with small amplitude:

$$\begin{aligned} x(s) &= s \\ y(s) &= -0.5\ sin(\pi s) - \alpha\ sin(50\pi s) \end{aligned}$$

where α is the noise amplitude. In Fig 1a we show the plot of $(x(T,s), y(T,s))$, at $T = .1$, which is the solution of the Cauchy-Riemann equations in Lagrangian coordinates for $\alpha = .005$. The equations were solved using a Lax-Friedrichs scheme and 200 points. The dissipation in the scheme was large enough in this case (or, equivalently, the mesh was coarse enough) to prevent roundoff noise from polluting the computation. The "loops" in the picture represent the growth of the initial noise. These loops grow exponentially in time, so for later times the computation explodes.

We solve the same initial value problem using the level set formulation given in (2.20), (2.21). We simplify the equations by setting

$$\begin{aligned} \varphi(t,x,y) &= y - \varphi(t,x) \\ J(t,x,y) &= J(t,x) \end{aligned}$$

and to get a system of conservation laws (which is a convenient system to approximate numerically), we further set

$$u = \varphi_x$$

and obtain

$$\begin{aligned} u_t - \left(\frac{1+u^2}{J}\right)_x &= 0 \\ J_t - u_x &= 0 \end{aligned} \tag{3.1}$$

The corresponding initial data is given by

$$\begin{aligned} u(0,x) &= -0.5\pi\ cos(\pi x) + \alpha 50\pi\ cos(50\pi x) \\ J(0,x) &= 1 \end{aligned} \tag{3.2}$$

The boundary conditions are periodic:

$$\begin{aligned} u(t,-1) &= u(t,1) \\ J(t,-1) &= J(t,1) \end{aligned}$$

We also add a curvature like regularization of the order of the mesh size to both equations:

$$\epsilon\Delta x \left(\frac{u_x\sqrt{1+u^2}}{J}\right)_x$$

with $\epsilon = .75$.

The numerical method we use to advect the system is a Lax-Friedrichs type scheme. In Fig 1b we show the solution $y = \varphi(T,x)$ at time $T = .1$ with 200 points. The function φ was obtained from u by integrating. Comparing with Fig 1a, the "loops" are not present and the solution curve has not changed its index.

In our second set of numerical experiments, we set the noise to zero ($\alpha = 0$). In this case the curve develops only one loop, at the point where the curve has a minimum. The solution is given analytically in (1.5). In Fig 2a,c,d we compare the analytic solution (solid curve) with the level set computation (circles) at different times in terms of the function $y = \varphi(T,x)$. In Fig 2b we have the

same solution as in Fig 2a, but in terms of $u(T,x)$ (top) and $J(T,x)$ (bottom). At T=.2, the exact solution is barely past the time of singularity.

We note that the numerical solution approximates very well the exact solution away from the singularity. Near the singularity, the numerical solution has preserved its index. From Fig 2b, it appears that the level set formulation admits a solution with a discontinuity in u and a delta function in J.

In the third and final set of experiments, we considered a different parametrization of the initial data to cause merging of different parts of the curve and a bubble to form. For example, we chose the following initial conditions for the Lagrangian formulation:

$$\begin{aligned} x(0,s)) &= s + sgn(s)\frac{cos(\pi s) - 1}{2\pi} \\ y(0,s) &= -.4 - .5sin\left(\frac{\pi}{1-1/\pi}x((0,s)\right) \end{aligned}$$

The graph of this curve is still a simple sinusoidal curve, but the parametrization makes the middle part move faster. The solution at a later time is given in Fig 3a. Notice that the curve has merged and self-intersected without a change in index. This solution was computed with a Lax-Friedrichs type scheme in Lagrangian coordinates, with a curvature regularization.

We computed a similar solution using the level set method. In order to be able to handle the change of topology, we computed the full two dimensional equations (2.20), (2.21) with a small curvature regularization. Since it is too complicated to find the initial data for the level set formulation that corresponds exactly to the Lagrangian data given above, we chose a similar but slightly different one. The level set solution is therefore not the same as the Lagrangian solution, but qualitatively similar.

The level set solutions are shown in Fig 3b-d at different times. After it merges, the curve forms a bubble which separates (Fig 3d). This is typical of the level set approach which does not allow self intersections. Notice that, even though both the Lagrangian and the level set equations use a curvature regularization, the results are qualitatively different.

The boundary conditions are: periodic J in both x and y, periodic φ in x and modulo 2 in y.

A. Appendix. We analyze the linearized stability of our system (2.15), (2.16). We have two main results. The first is that the linearized problem (2.15, (2.16) is well posed iff the original problem (1.1) has that property. The second is that the linearized problem is always well posed in the direction normal to level sets of φ. In fact it is precisely (2.15), (2.16) with a "frozen" value of the vector v.

The linearized version of problem (1.1) is (up to lower order terms)

$$\text{(A.1)} \qquad \begin{pmatrix} x_t \\ y_t \end{pmatrix} = \begin{pmatrix} (v_1)_{x_s} & (v_1)_{y_s} \\ (v_2)_{x_s} & (v_2)_{y_s} \end{pmatrix} \begin{pmatrix} x_s \\ y_s \end{pmatrix}$$

This is well posed (hyperbolic) iff

$$\text{(A.2)} \qquad ((v_1)_{x_s} - (v_2)_{y_s})^2 > -4(v_1)_{y_s}(v_2)_{x_s}.$$

We may rotate coordinates in equation (2.15) locally and assume that φ is the graph of a function, i.e.:

$$\text{(A.3)} \qquad \begin{aligned} \varphi(x,y,t) &= T(x,t) - y \\ \psi(x,y,t) &= \psi(x,T(x,t),t) = \psi(x,t). \end{aligned}$$

(the second equation follows by defining $\psi(x,T(x,t),t) = \psi(x,t)$).
Then

$$\text{(A.4)} \qquad \begin{aligned} x_s &= \frac{1}{\psi_x} \\ y_s &= \frac{T_x}{\psi_x}. \end{aligned}$$

Equations (2.15), (2.16) becomes (suppressing the t,x,y dependence in v_1, v_2):

$$\text{(A.5)} \qquad \begin{aligned} T_t &+ v_1\left(\frac{1}{\psi_x}, \frac{T_x}{\psi_x}\right) T_x - v_2\left(\frac{1}{\psi_x}, \frac{T_x}{\psi_x}\right) = 0 \\ \psi_t &+ v_1\left(\frac{1}{\psi_x}, \frac{T_x}{\psi_x}\right) \psi_x = 0 \end{aligned}$$

The linearized problem, modulo lower order terms is:

$$\begin{pmatrix} T_t \\ \varphi_t \end{pmatrix} + A \begin{pmatrix} T_x \\ \varphi_x \end{pmatrix} = 0 \tag{A.6}$$

where

$$A = \begin{bmatrix} (v_1 + (v_1)_{y_s}\frac{T_x}{\psi_x} - (v_2)_{y_s}\frac{1}{\psi_x}) & -(v_1)_{x_s}\frac{T_x}{\psi_x^2} - (v_1)_{y_s}\frac{T_x^2}{\psi_x^2} \\ & +(v_2)_{x_s}\frac{1}{\psi_x^2} + (v_2)_{y_s}\frac{T_x}{\psi_x^2} \\ (v_1)_{y_s} & v_1 - (v_1)_{x_s}\frac{1}{\psi_x} - (v_1)_{y_s}\frac{T_x}{\psi_x} \end{bmatrix}. \tag{A.7}$$

This is well-posed iff

$$\begin{aligned} \left[(v_1)_{y_s}\frac{2T_x}{\psi_x} - \frac{(v_2)_{y_s} - (v_1)_{x_s}}{\psi_x}\right]^2 \quad &> \quad -4(v_1)_{y_s}(-(v_1)_{x_s}\frac{T_x}{\psi_x^2} \\ &- \quad (v_1)_{y_s}\frac{T_x^2}{\psi_x^2} + (v_2)_{x_s}\frac{1}{\psi_x^2} + (v_2)_{y_s}\frac{T_x}{\psi_x^2}) \end{aligned} \tag{A.8}$$

or iff

$$((v_2)_{y_s} - (v_1)_{x_s}^2)^2 > -4(v_1)_{y_s}(v_2)_{x_s}. \tag{A.9}$$

Thus, we have proven.

THEOREM A.1. *The linearized version of problem (1.1) is well posed iff the linearized version of the level set extension (2.15) is well posed.*

Next we linearize (2.15), (2.16) arriving (modulo lower order terms) at the system

$$\begin{pmatrix} \varphi \\ \psi \end{pmatrix}_t + A \begin{pmatrix} \varphi \\ \psi \end{pmatrix}_x + B \begin{pmatrix} \varphi \\ \psi \end{pmatrix}_y = 0. \tag{A.10}$$

We wish to show that the matrix $(A\xi + B\eta)$ has real distinct eigenvalues for $\xi = \varphi_x$, $\eta = \varphi_y$. Here

$$B\eta = \begin{pmatrix} (v_1\xi + v_2\eta) + \varphi_x(\xi(v_1)_{\varphi_x} + \eta(v_1)_{\varphi_y}) & \varphi_x(\xi(v_1)_{\psi_x} + \eta(v_1)_{\psi_y}) \\ +\varphi_y(\xi(v_2)_{\varphi_x} + \eta(v_2)_{\varphi_y}) & +\varphi_y(\xi(v_2)_{\psi_x} + \eta(v_2)_{\psi_y}) \\ \psi_x(\xi(v_1)_{\varphi_x} + \eta(v_1)_{\varphi_y}) & (v_1\xi + v_2\eta) + \psi_x(\xi(v_1)_{\psi_x} + \eta(v_1)_{\psi_y}) \\ +\psi_y(\xi(v_2)_{\varphi_x} + \eta(v_2)_{\varphi_y}) & +\psi_y(\xi(v_2)_{\psi_x} + \eta(v_2)_{\psi_y}) \end{pmatrix}. \tag{A.11}$$

We now show:

$$A\varphi_x + B\varphi_y = (v_1\varphi_x + v_2\varphi_y)I. \tag{A.12}$$

This is equivalent to showing (via the chain rule) that

$$\varphi_x(x_s)\varphi_x + \varphi_y(x_s)\varphi_y = 0 \tag{A.13}$$

$$\varphi_x(y_s)\varphi_x + \varphi_y(y_s)\varphi_y = 0 \tag{A.14}$$

$$\varphi_x(x_s)\psi_x + \varphi_y(x_s)\psi_y = 0 \tag{A.15}$$

$$\varphi_y(y_s)\psi_x + \varphi_y(y_s)\psi_y = 0. \tag{A.16}$$

Since x_s and y_s are homogeneous of degree zero in (φ_x, φ_y), (see 2.14), equations (A.14) and (A.15) come immediately from differentiating the identities

$$x_s(c\varphi_x, c\varphi_y) \equiv x_s(\varphi_x, \varphi_y) \tag{A.17}$$

$$y_s(c\varphi_x, c\varphi_y) \equiv y_s(\varphi_x, \varphi_y) \tag{A.18}$$

with respect to c, then setting $c = 1$.

Next, the formula in (2.14) are of the form

$$x_s = -f(\varphi_x\psi_y - \varphi_y\psi_x)\varphi_y \tag{A.19}$$

$$y_s = f(\varphi_x\varphi_y - \varphi_y\psi_x)\varphi_x \tag{A.20}$$

and (A.15), (A.16) follow immediately. We thus have:

THEOREM A.2. *The linearized problem (2.15), (2.16), up to lower order terms, evaluated in the direction (φ_x, φ_y) is just the simple decoupled system (2.15), (2.16) with the velocity vector $\vec{v}$ frozen at its linearized value*

REFERENCES

[1] L. Alvarez, F. Guichard, P.-L. Lions, and J.-M. Morel, *Axioms and fundamental equations of image processing*, Arch. Rat. Mech. and Analysis, 123 (1993), pp. 199–258.

[2] S. Chen, B. Merriman, S. Osher, and P. Smereka, *A simple level set based algorithm for solving Stefan problems*, UCLA CAM Report 96-21, submitted to J. Comput. Phys. (1996).

[3] Y. G. Chen, Y. Giga, and S. Goto, *Uniqueness and existence of viscosity solutions of generalized mean curvature flow equations*, J. Diff. Geom., 33 (1991), pp. 749–786.

[4] D. Chopp, *Computing minimal surfaces via level set curvature flow*, J. Comput. Phys., 106 (1993), pp. 77–91.

[5] L. C. Evans and J. Spruck, *Motion of level sets by mean curvature*, J. Diff. Geom., 33 (1994), pp. 635–681.

[6] E. Harabetian, S. Osher, and C.-W. Shu, *An Eulerian approach for vortex motion*, J. Comput. Phys., 127 (1996), pp. 15–26.

[7] T.-Y. Hou, *Numerical solutions to free boundary problems*, Acta Numerica, (1995), pp. 335–415.

[8] T.-Y. Hou, J. Lowengrub, and M. Shelley, *Removing the stiffness from interfacial flows with surface tension*, J. Comput. Phys., 114 (1994), pp. 312–338.

[9] B. Merriman, J. Bence, and S. Osher, *Motion of multiple junctions, a level set approach*, J. Comput. Phys., 112 (1994), pp. 334–363.

[10] R. E. Meyer, *Introduction to mathematical fluid dynamics*, Wiley-Interscience, New York, 1971.

[11] S. Osher, *A level set formulation for the solution of the Dirichlect problem for Hamilton-Jacobi equations*, SIAM J. on Anal., 24 (1993), pp. 1145–1152.

[12] S. Osher and J. A. Sethian, *Fronts propagating with curvature dependent speed*, J. Comput. Phys., 79 (1988), pp. 12–49.

[13] S. Osher and C.-W. Shu, *High-order essentially nonoscillatory schemes for Hamilton-Jacobi equations*, SINUM, 28 (1991), pp. 907–922.

[14] L. Rudin and S. Osher, *Total variation based restoration with free local constraints*, Proceedings ICIP, 1994, IEEE Int. Conf. on Image Processing, 1994, Austin, TX, pp. 31–35.

[15] L. Rudin, S. Osher, and E. Fatemi, *Nonlinear total variation based noise removal algorithms*, Physica D, 60 (1992), pp. 259–268.

[16] J. A. Sethian, *Curvature and the evolution of fronts*, Comm. Math. Phys., 101 (1985), pp. 487–499.

[17] M. Sussman, P. Smereka, and S. Osher, *A level set approach for computing solutions to incompressible two-phase flow*, J. Comput. Phys., 114 (1994), pp. 146–159.

[18] H. K. Zhao, T. Chan, B. Merriman, and S. Osher, *A variational level set approach to multiphase motion*, J. Comput. Phys., 127 (1996), pp. 179–195.

[19] J. Zhu and P. Ronney, *Non-dimensional flow distribution intensities*, Combustion Science and Technology (1994), to appear.

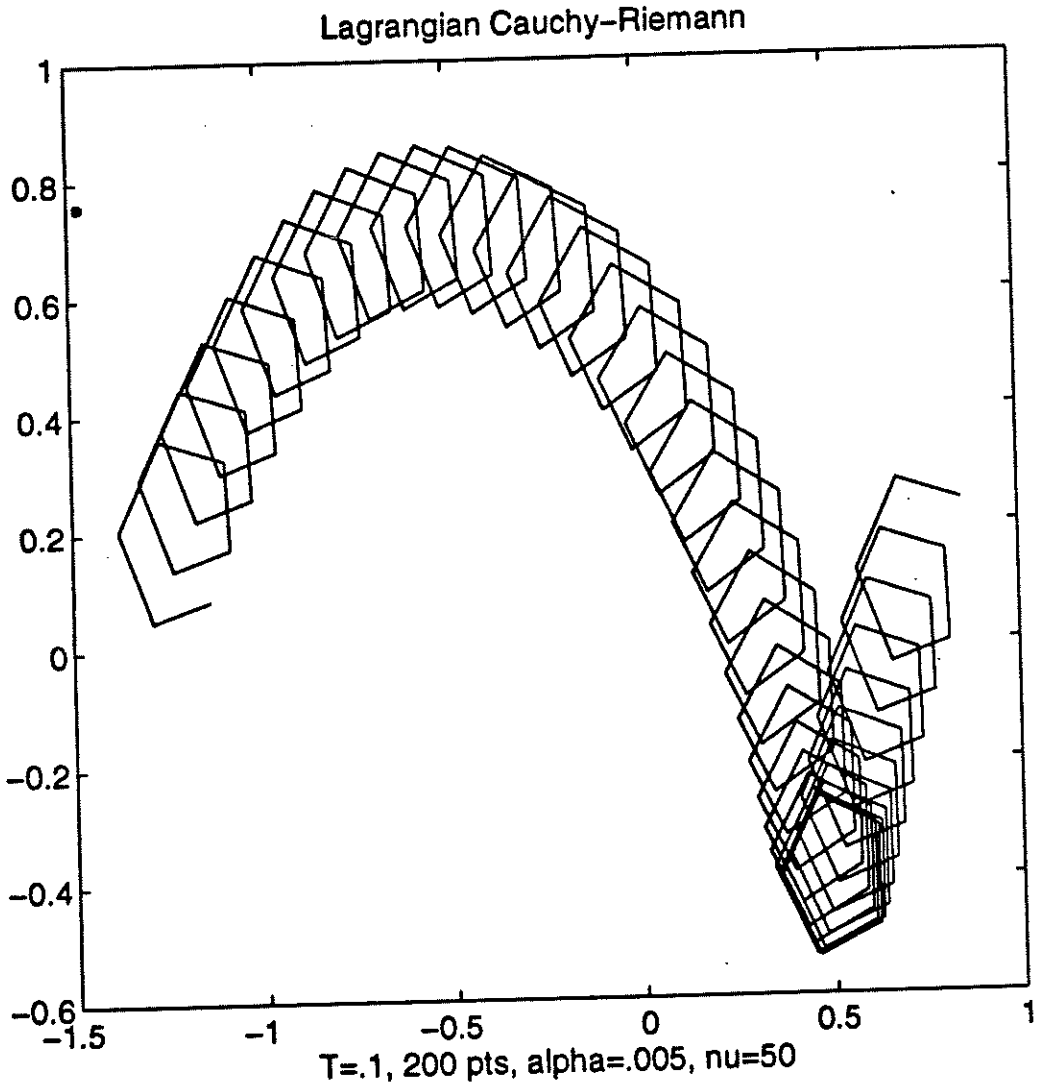

Figure 1a: $(x(T,s), y(T,s))$ graph of solution to Cauchy Riemann equations with noisy initial data

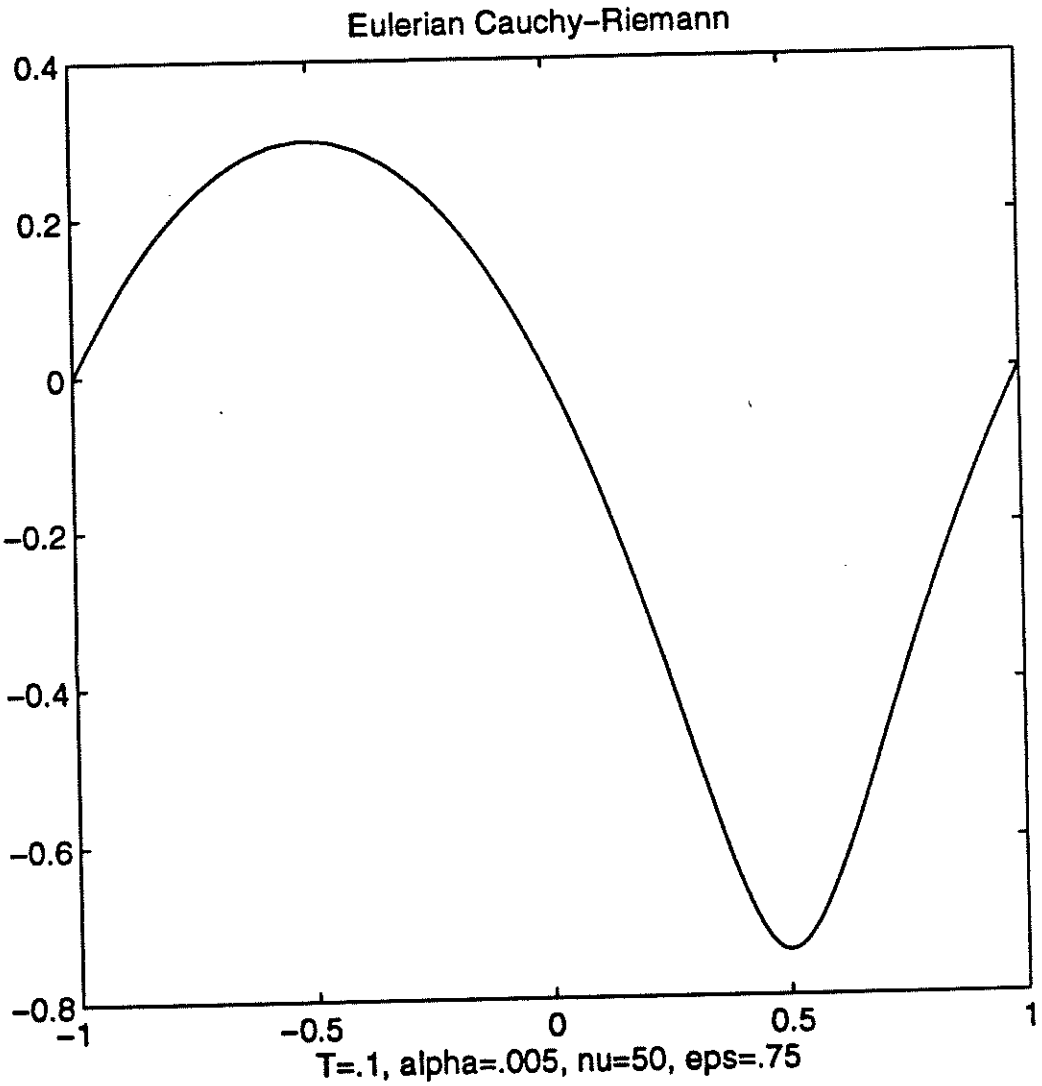

Figure 1b: Level set solution to Cauchy-Riemann equations with noisy initial data

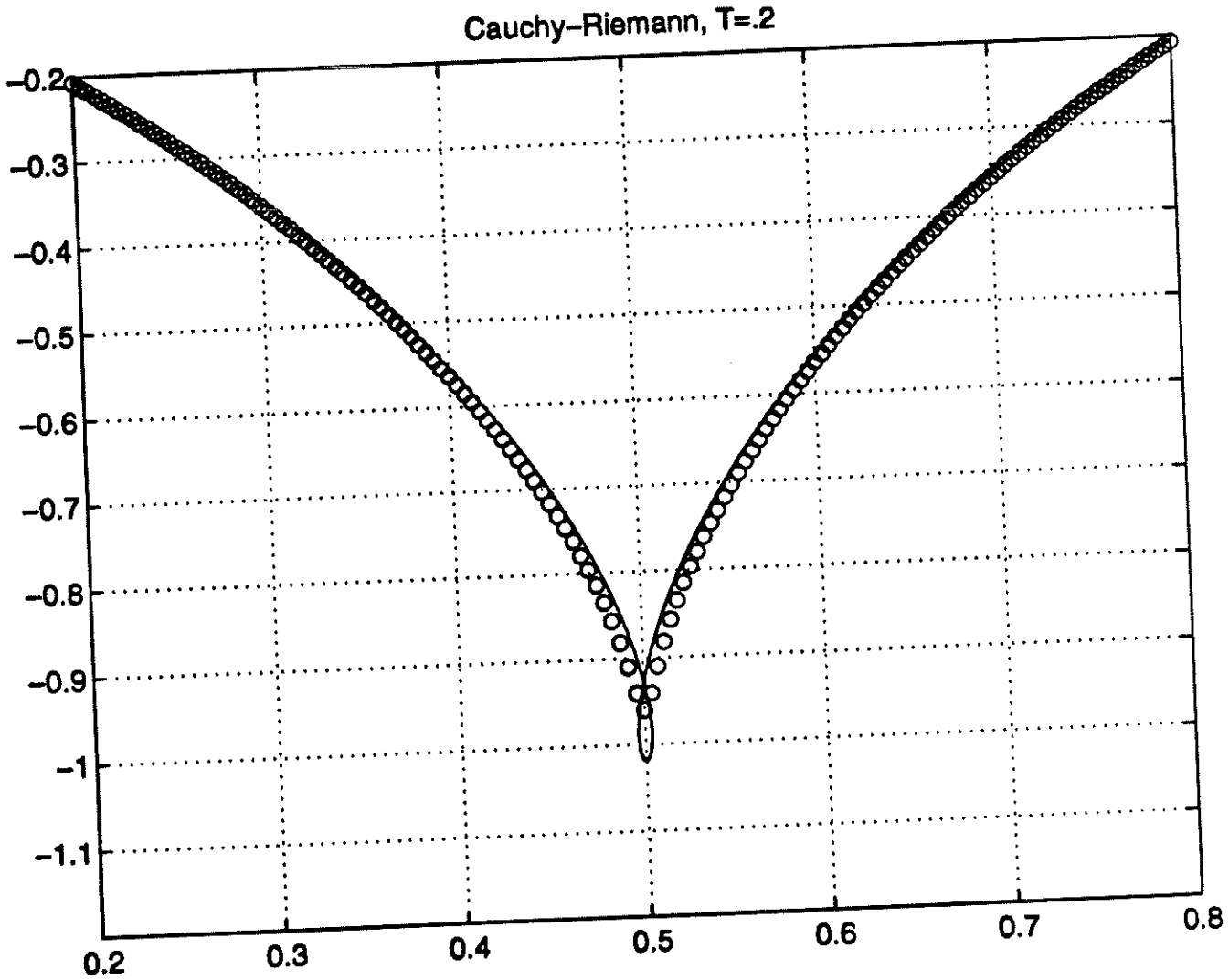

Figure 2a: Analytic solution (solid line) compared to level set computation just after time of singularity

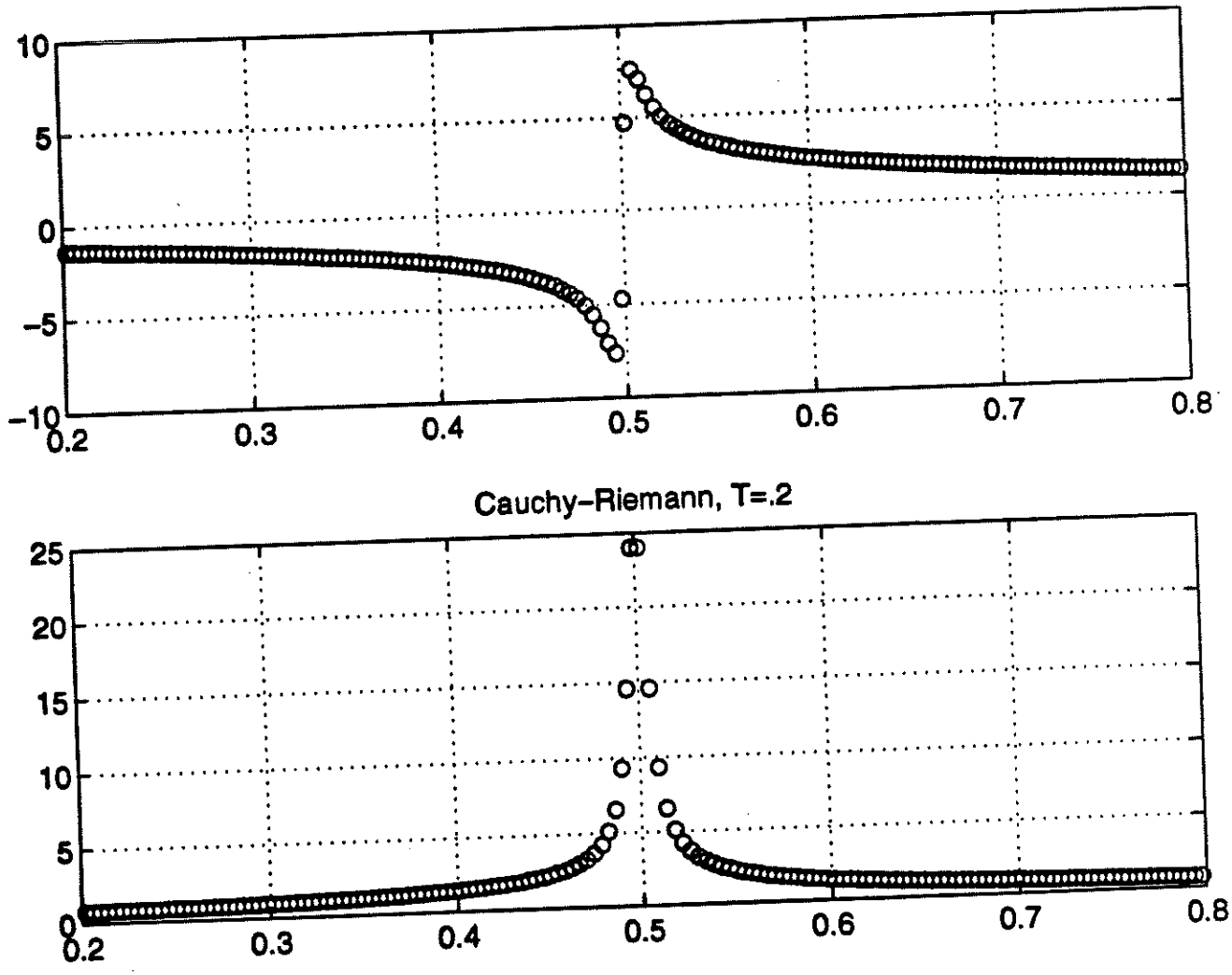

Figure 2b: "Shock" in $u(T,x)$ just after time of singularity (top)
"delta function" in $J(T,x)$ just after time of singularity (bottom)

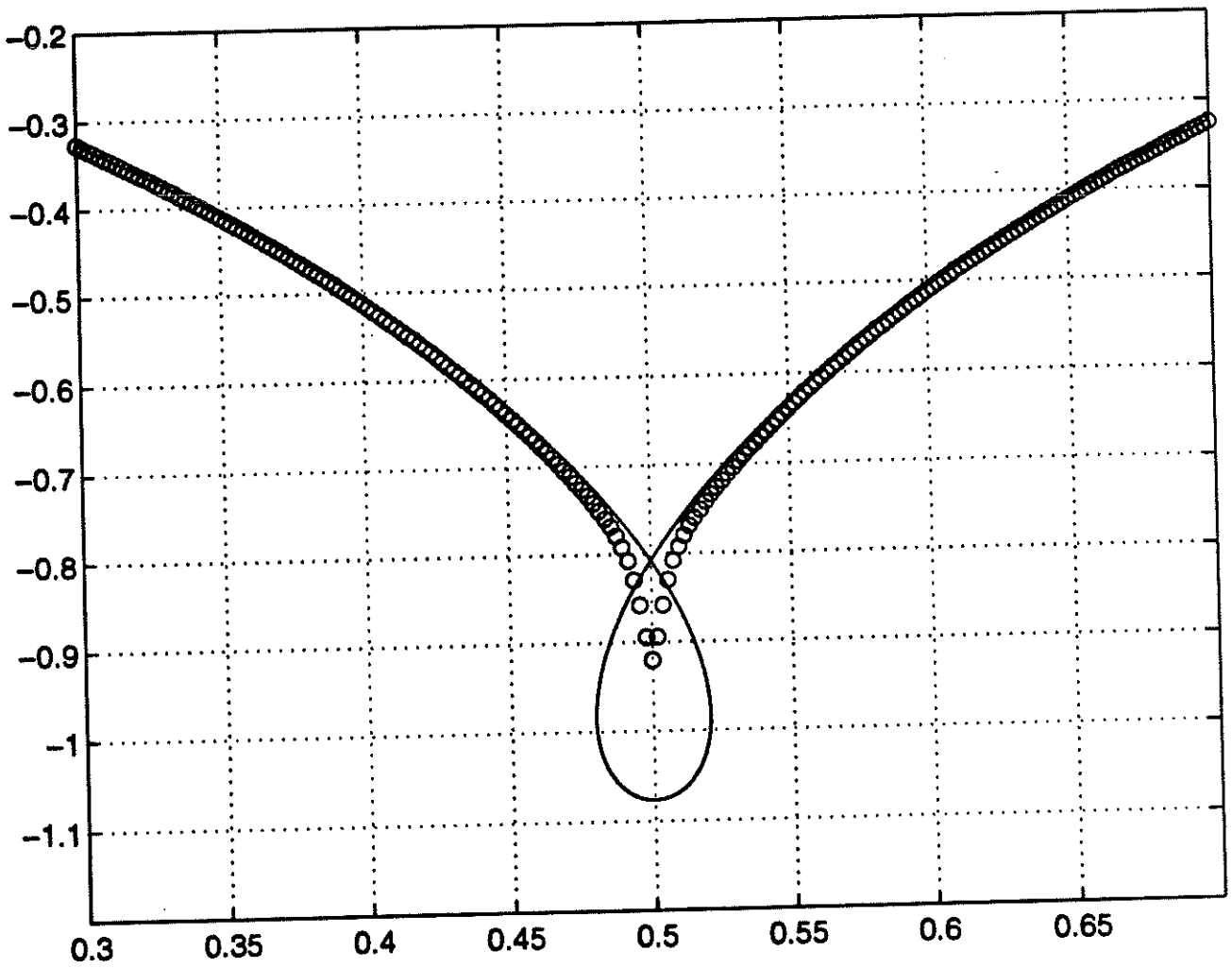

Figure 2c: Analytic solution (solid line) compared to level set computation at $T = .25$

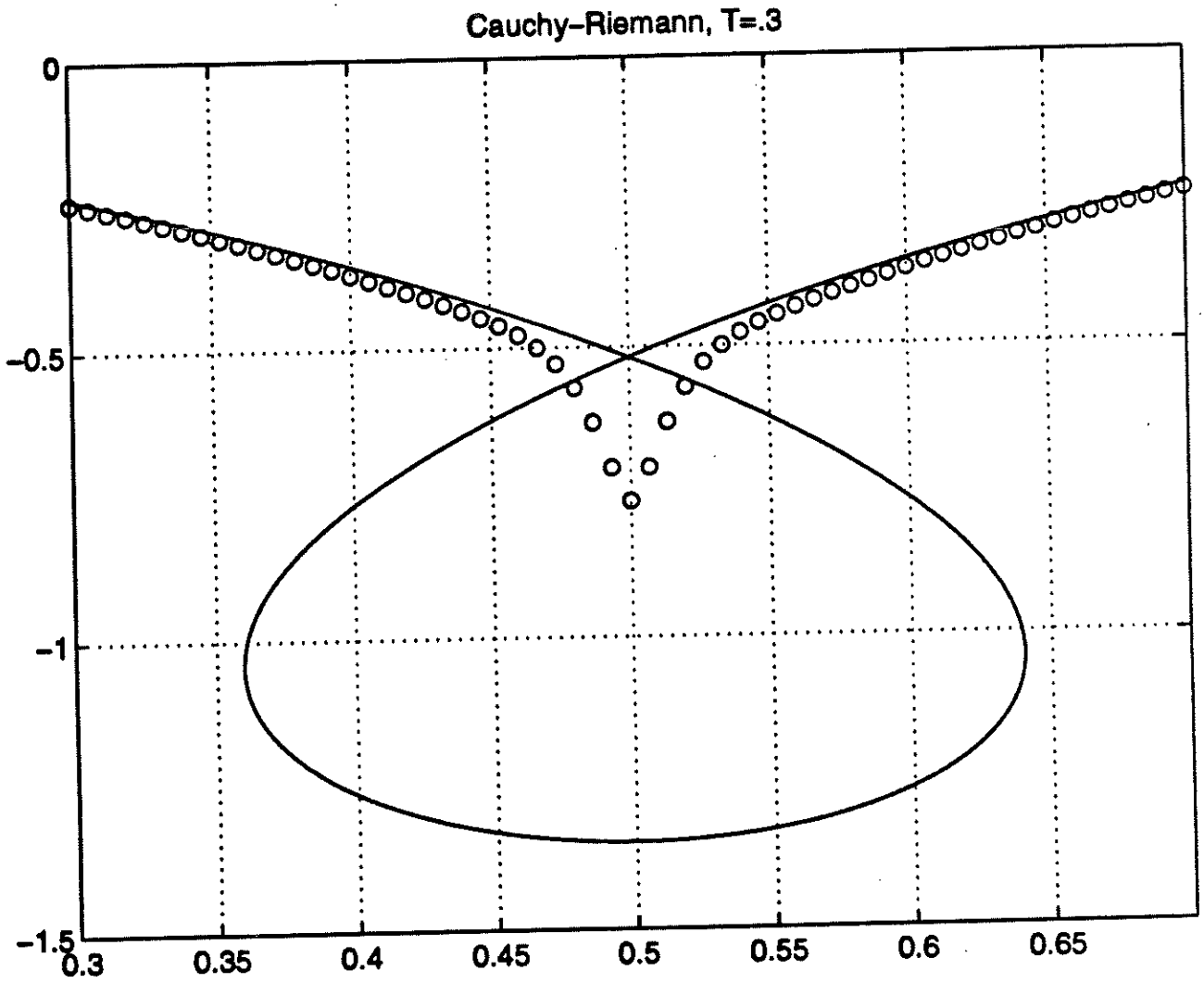

Figure 2d: Analytic solution (solid line) compared to level set computation at $T = .3$

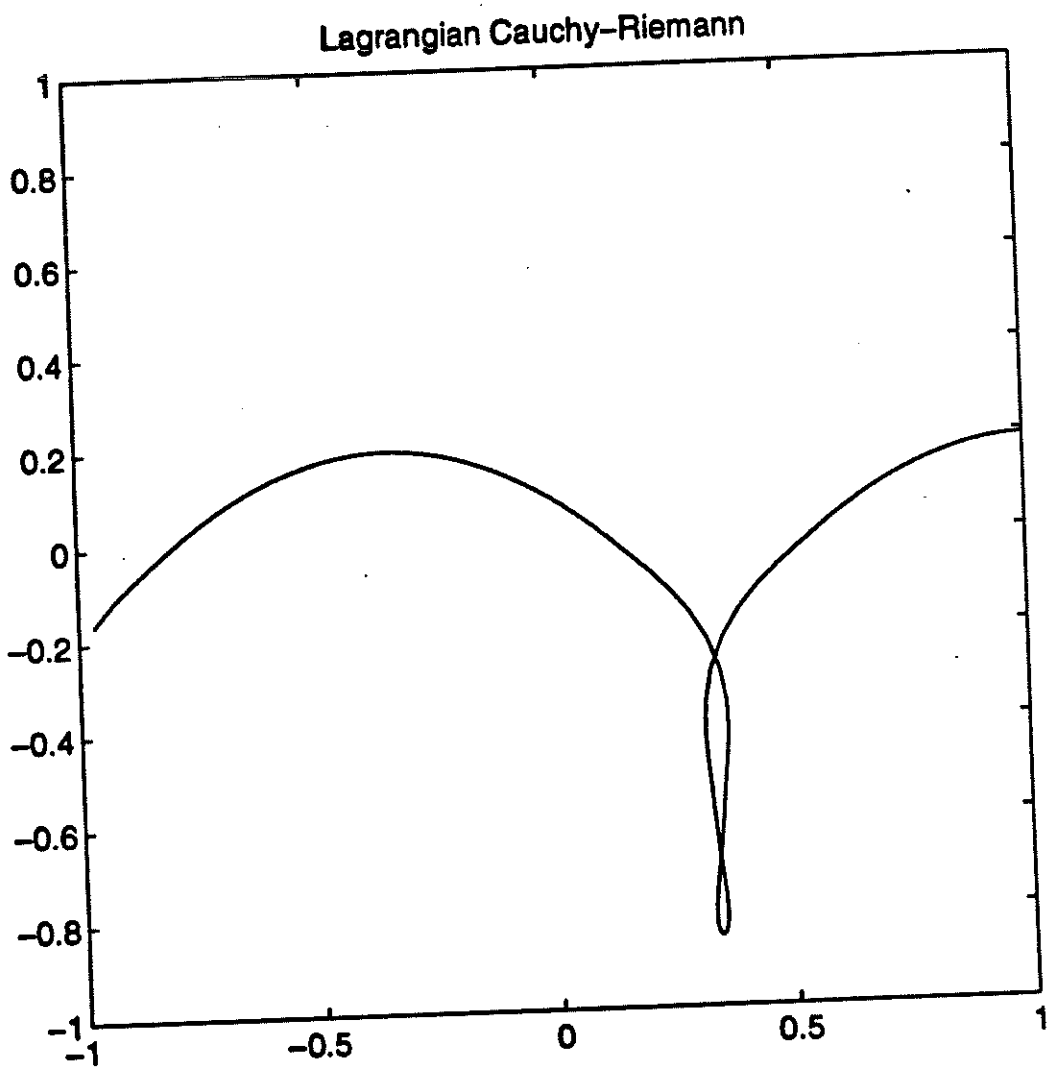

Figure 3a: Lagrangian computation of "figure eight".

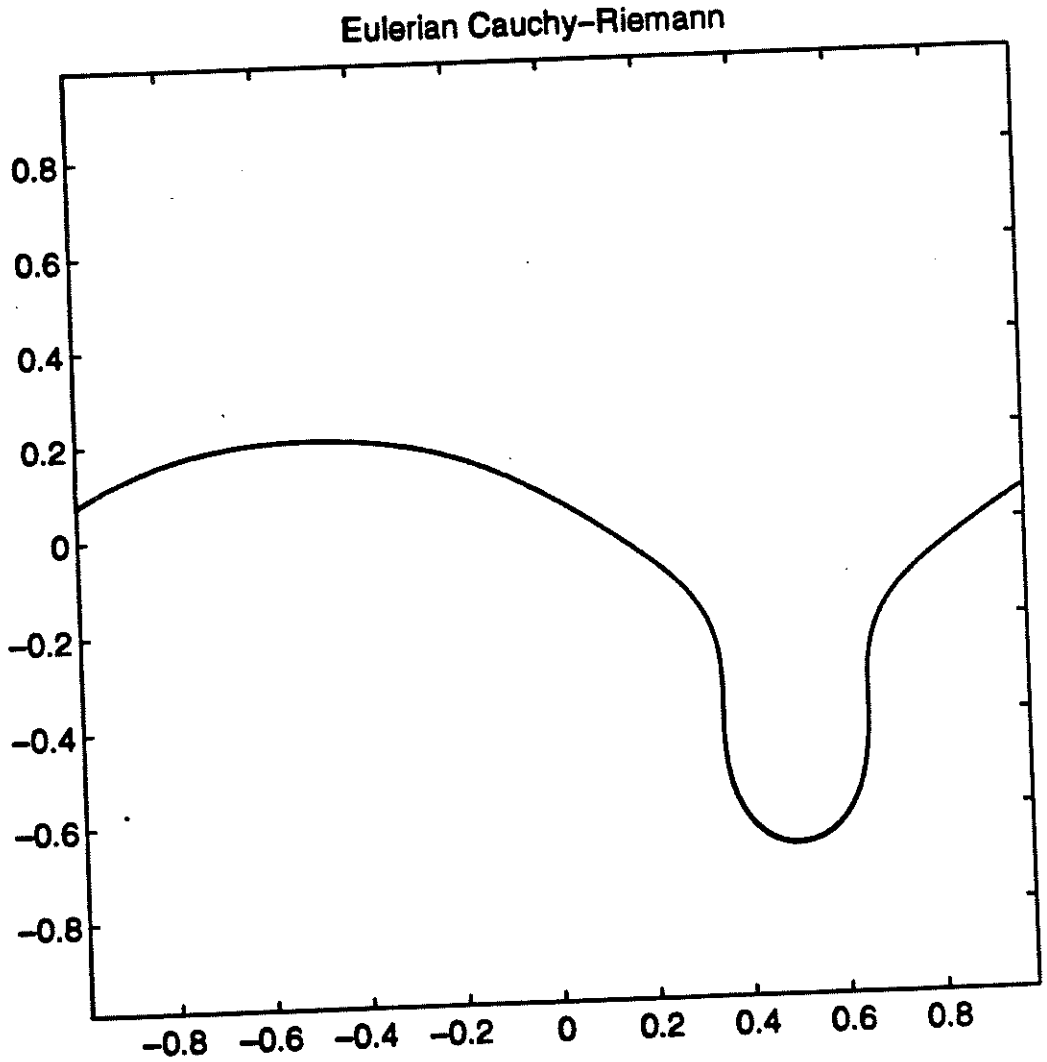

Figure 3b: Level set computation of development of bubble.
The middle part will move faster.

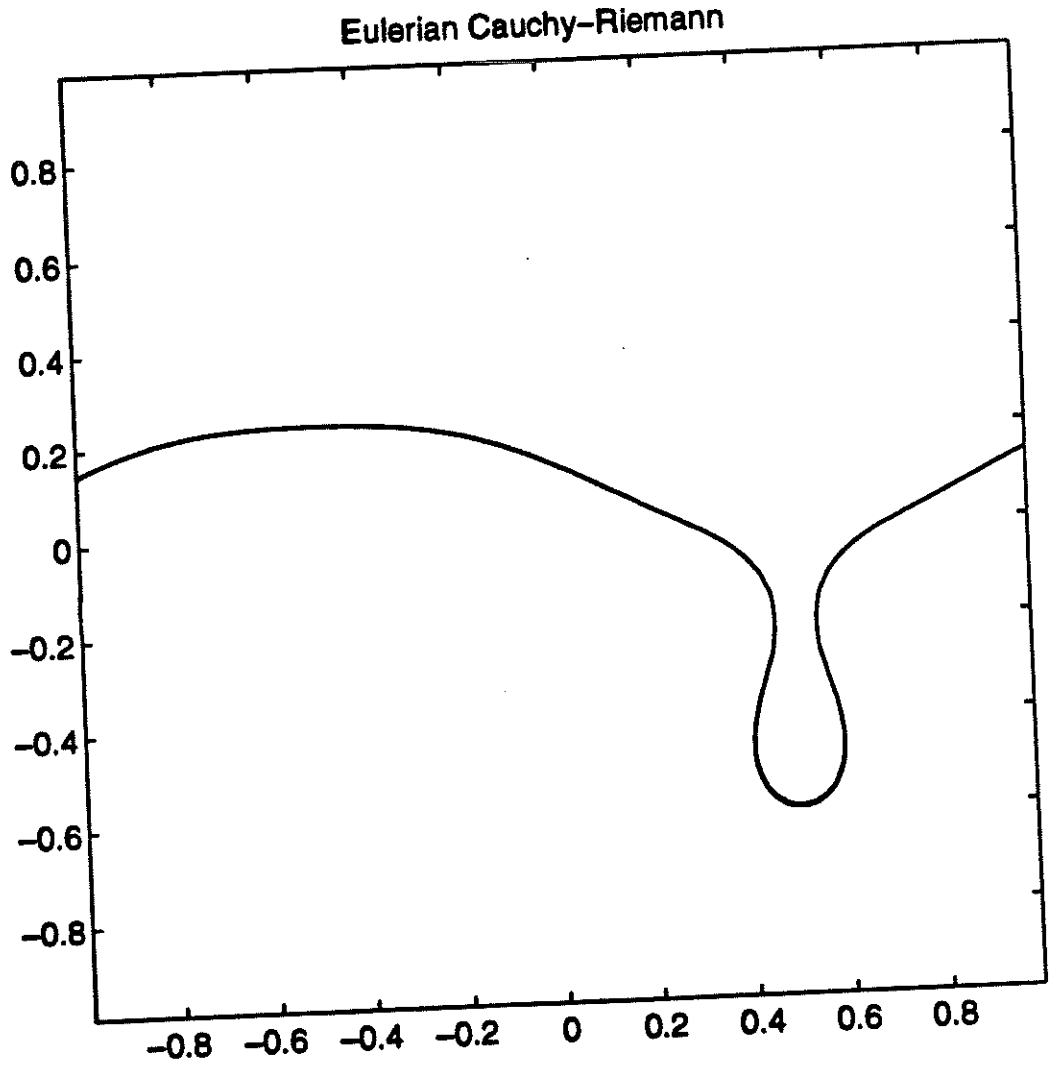

Figure 3c: Level set computation of develpment of bubble.
The middle part will tend to merge.

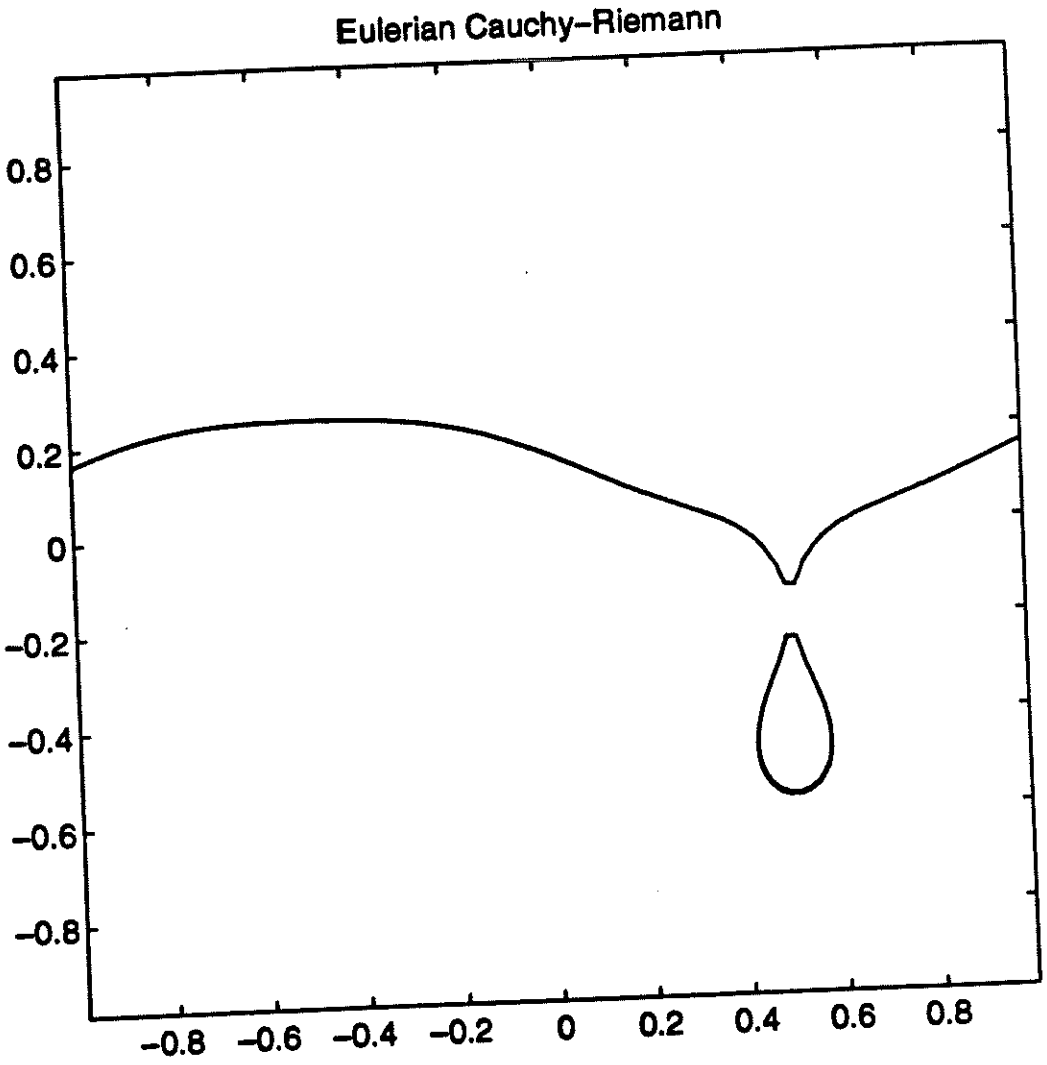

Figure 3d: Level set computation of development of bubble after pinchoff.